PNAS RESEARCH ARTICLE | BIOCHEMISTRY

ALS-linked C9orf72–SMCR8 complex is a negative regulator of primary ciliogenesis

Dan Tang[a,1], Kaixuan Zheng[a,1], Jiangli Zhu[a,b,1], Xi Jin[a,1], Hui Bao[a,1], Lan Jiang[a,1], Huihui Li[a], Yichang Wang[a,c], Ying Lu[a], Jiaming Liu[a], Hang Liu[d,e,f], Chengbing Tang[a], Shijian Feng[a], Xiuju Dong[a], Liangting Xu[a], Yike Yin[a], Shangyu Dang[d,e,f], Xiawei Wei[c], Haiyan Ren[a], Biao Dong[c,g], Lunzhi Dai[a], Wei Cheng[a], Meihua Wan[a], Zhonghan Li[a], Jing Chen[a], Hong Li[a], Eryan Kong[b,2], Kunjie Wang[a,2], Kefeng Lu[a,2], and Shiqian Qi[a,h,2]

Edited by Li Yu, Tsinghua University, Beijing, China; received December 2, 2022; accepted October 25, 2023 by Editorial Board Member Nieng Yan

Massive GGGGCC (G4C2) repeat expansion in *C9orf72* and the resulting loss of C9orf72 function are the key features of ~50% of inherited amyotrophic lateral sclerosis and frontotemporal dementia cases. However, the biological function of C9orf72 remains unclear. We previously found that C9orf72 can form a stable GTPase activating protein (GAP) complex with SMCR8 (Smith-Magenis chromosome region 8). Herein, we report that the C9orf72–SMCR8 complex is a major negative regulator of primary ciliogenesis, abnormalities in which lead to ciliopathies. Mechanistically, the C9orf72–SMCR8 complex suppresses the primary cilium as a RAB8A GAP. Moreover, based on biochemical analysis, we found that C9orf72 is the RAB8A binding subunit and that SMCR8 is the GAP subunit in the complex. We further found that the C9orf72–SMCR8 complex suppressed the primary cilium in multiple tissues from mice, including but not limited to the brain, kidney, and spleen. Importantly, cells with C9orf72 or SMCR8 knocked out were more sensitive to hedgehog signaling. These results reveal the unexpected impact of C9orf72 on primary ciliogenesis and elucidate the pathogenesis of diseases caused by the loss of C9orf72 function.

C9orf72 | SMCR8 | primary cilium | GAP | membrane trafficking

Significance

Loss of C9orf72 function caused by the abnormal GGGGCC (G4C2) repeat expansion in *C9orf72* might exacerbate amyotrophic lateral sclerosis (ALS) and frontotemporal dementia (FTD). However, the biological function of C9orf72 remains unclear. Here, we report that the C9orf72–SMCR8 (Smith-Magenis chromosome region 8) complex suppresses primary cilium growth as a RAB8A GAP (GTPase activating protein), establishing a link between C9orf72 function and the primary cilium and hedgehog signaling. This discovery sheds light on a potential pathogenic mechanism related to the loss of C9orf72 function.

The massive expansion of GGGGCC (G4C2) repeats in the first intron of *C9orf72* causes ~50% of genetic cases of amyotrophic lateral sclerosis (ALS) and frontotemporal dementia (FTD) (1, 2). Two major mechanisms, gain of toxicity and loss of function, have been proposed to explain the pathophysiology of *C9orf72*-ALS (1–4). The gain of toxicity is attributed to the accumulation of poly-dipeptides and RNA G-quadruplexes derived from massive G4C2 repeats (5, 6). Moreover, loss of function resulting from decreases in the transcription and expression of *C9orf72* exacerbates the outcomes resulting from the gain of toxicity (4, 7, 8). Although many substantial studies have suggested that C9orf72 plays a critical role in regulating autophagy (9, 10), lysosome function (11, 12), immune responses (13, 14), synaptic function (15, 16), and membrane trafficking (17–19), the specific physiological function of C9orf72 remains elusive.

C9orf72, Smith-Magenis chromosome region 8 (SMCR8), and WDR41 can form a stable functional complex that regulates multiple biological processes in cells (9, 20). Both C9orf72 and SMCR8 are members of the differentially expressed in normal and neoplastic cells family (17, 21), the members of which are well-characterized as guanine nucleotide exchange factors (GEFs) for RAB GTPases (22, 23). C9orf72 has also been implicated in the regulation of autophagy and membrane trafficking via its GEF function for many RABs, such as RAB8A, RAB29, and RAB39B (9, 24). However, structural analyses have revealed that the C9orf72–SMCR8 complex shows an overall structural fold similar to that of the FLCN–FNIP2 complex, which regulates mTOR1 signaling as a GTPase activating protein (GAP) for RRAGC/D (18, 19, 25, 26). Besides, both structural and bioinformatic analyses have suggested that Arg147 of SMCR8 corresponds to the arginine finger of FLCN, indicating that the C9orf72–SMCR8 complex might function as a GAP in some signaling pathways (18, 19). Biophysical and biochemical experiments revealed that the C9orf72–SMCR8 complex is a GAP for RAB8A (18, 27), RAB11A (18, 27), and ARF1 (19, 28) and that Arg147 of SMCR8 is critical for its GAP activity in vitro (18, 19, 28).

RAB8A is a member of the RAB family that is critical for vesicle biogenesis, trafficking, tethering, and fusion (29, 30). Specifically, RAB8A plays critical roles in intercellular communication (31, 32), apical transportation (33, 34), exocytosis (35), axon growth (36), and primary ciliogenesis (37, 38). The primary cilium, a single, nonmotile, microtubule-based organelle that is present on the surface of most cell types in humans, is the key regulator of homeostasis and development (39–41). Generally, the BBSome,

Author contributions: D.T., K.Z., J.Z., X.J., H.B., L.J., Y.Y., S.D., M.W., Z.L., E.K., K.W., K.L., and S.Q. designed research; D.T., K.Z., J.Z., X.J., H.B., L.J., Y.W., H. Liu, C.T., S.F., X.D., L.X., and Y.Y. performed research; Y.L., B.D., L.D., Z.L., J.C., E.K., and K.W. contributed new reagents/analytic tools; D.T., K.Z., J.Z., X.J., H.B., L.J., Huihui Li, Y.W., Y.L., J.L., H. Liu, Y.Y., S.D., X.W., H.R., B.D., L.D., W.C., M.W., Z.L., Hong Li, E.K., K.W., K.L., and S.Q. analyzed data; and D.T., H.B., S.D., Z.L., E.K., K.L., and S.Q. wrote the paper.

Competing interest statement: B.D. is a founder and the president of Sichuan Real & Best Biotech Co., Ltd. S.Q. is a consultant for Sichuan Real & Best Biotech Co., Ltd.

This article is a PNAS Direct Submission. L.Y. is a guest editor invited by the Editorial Board.

[1]D.T., K.Z., J.Z., X.J., H.B., and L.J. contributed equally to this work.

[2]To whom correspondence may be addressed. Email: eykong2012@163.com, wangkj@scu.edu.cn, lukf@scu.edu.cn, or qishiqian@scu.edu.cn.

This article contains supporting information online at https://www.pnas.org/lookup/suppl/doi:10.1073/pnas.2220496120/-/DCSupplemental.

Published December 8, 2023.

a protein complex related to Bardet–Biedl syndrome, is critical for primary ciliogenesis (42). The BBSome can recruit Rabin8 via its C-terminal tail to the primary cilium, where Rabin8 activates RAB8A as a GEF (42). Once activated by Rabin8, RAB8A promotes the assembly and elongation of the ciliary membrane by enhancing vesicle trafficking for primary ciliogenesis (43, 44). The primary cilium functions as an antenna to sense changes in the extracellular environment, including changes in light, signaling molecules, and mechanical stimuli (45, 46). Noteworthily, the primary cilium is fundamentally critical for hedgehog (Hh) signaling, which is essential for embryonic development and tissue homeostasis in vertebrates (47, 48). Dysfunction of the primary cilium results in many serious diseases that are referred to as ciliopathies, which manifest in patients as a wide spectrum of disorders, including congenital heart disease (49), cystic kidney disease (50, 51), and neurodegenerative diseases (52). Notably, either the loss of C9orf72 or dysfunction of the primary cilium can lead to neurodegenerative diseases and alterations in inflammatory responses (53, 54). However, the relationship between C9orf72 and the primary cilium has never been investigated.

In this manuscript, we demonstrated that the C9orf72–SMCR8 complex functions as a RAB8A GAP in cells to negatively regulate primary cilium growth and found that cells with knockout either C9orf72 or SMCR8 were more sensitive to sonic hh (Shh) stimulation. Moreover, we also reveal the structural and biochemical underpinnings by which the C9orf72–SMCR8 complex recognizes RAB8A and stimulates Guanosine-5'-triphosphate (GTP) hydrolysis. Our data thus reveal the role of C9orf72 in regulating the primary cilium, a key organelle at the plasma membrane (PM), and Hh signaling, which sheds light on the potential pathogenic mechanism related to the loss of C9orf72 function.

Results

The C9orf72–SMCR8 Complex Suppresses Primary Ciliogenesis. The RAB8A–RAB11A cascade has been suggested to play a pivotal role in primary ciliogenesis (38), and data from our previous study indicated that the C9orf72–SMCR8 complex is a RAB8A/11A GAP (18, 27). Therefore, to explore whether the C9orf72–SMCR8 complex affects primary ciliogenesis, we knocked out C9orf72 and SMCR8 in human HEK293T cells and APRE-19 cells (*SI Appendix*, Fig. S1 *A* and *B*). ARL13B (55) and acetylated tubulin (Ac-tubulin) (38) are usually used as markers of the primary cilium. We first evaluated whether ARL13B and Ac-tubulin could be used as primary cilium markers in C9orf72-knockout (C9KO) cells and SMCR8-knockout (S8KO) cells. Immunofluorescence staining showed that ARL13B and Ac-tubulin overlapped well in the primary cilia of wild-type (WT) cells, C9KO cells, and S8KO cells (*SI Appendix*, Fig. S1*C*), suggesting that neither C9orf72 knockout nor SMCR8 knockout affected the localization of ARL13B or Ac-tubulin in primary cilia. Because we performed many cotransfection experiments and used multiple fluorescence markers, in the following experiments, we mainly used ARL13B as the primary cilium marker.

Immunofluorescence staining showed that the average incidence of spontaneous primary ciliogenesis was significantly higher in both C9KO cells and S8KO cells than in WT cells (Fig. 1 *A*–*D*). Moreover, under serum-starvation conditions, the percentage of ciliated cells increased dramatically in C9KO cells and S8KO cells compared with WT cells (Fig. 1 *A*–*D*). We also measured the primary cilium length in cells cultured with or without serum. Both C9KO and S8KO cells exhibited primary cilia with an increased average length (Fig. 1 *A*–*D*). Consistently, overexpressing C9orf72 or SMCR8 inhibited primary ciliogenesis (*SI Appendix*, Fig. S2 *A*–*D*). Notably, these phenotypes caused by C9KO or S8KO could be rescued by overexpression of

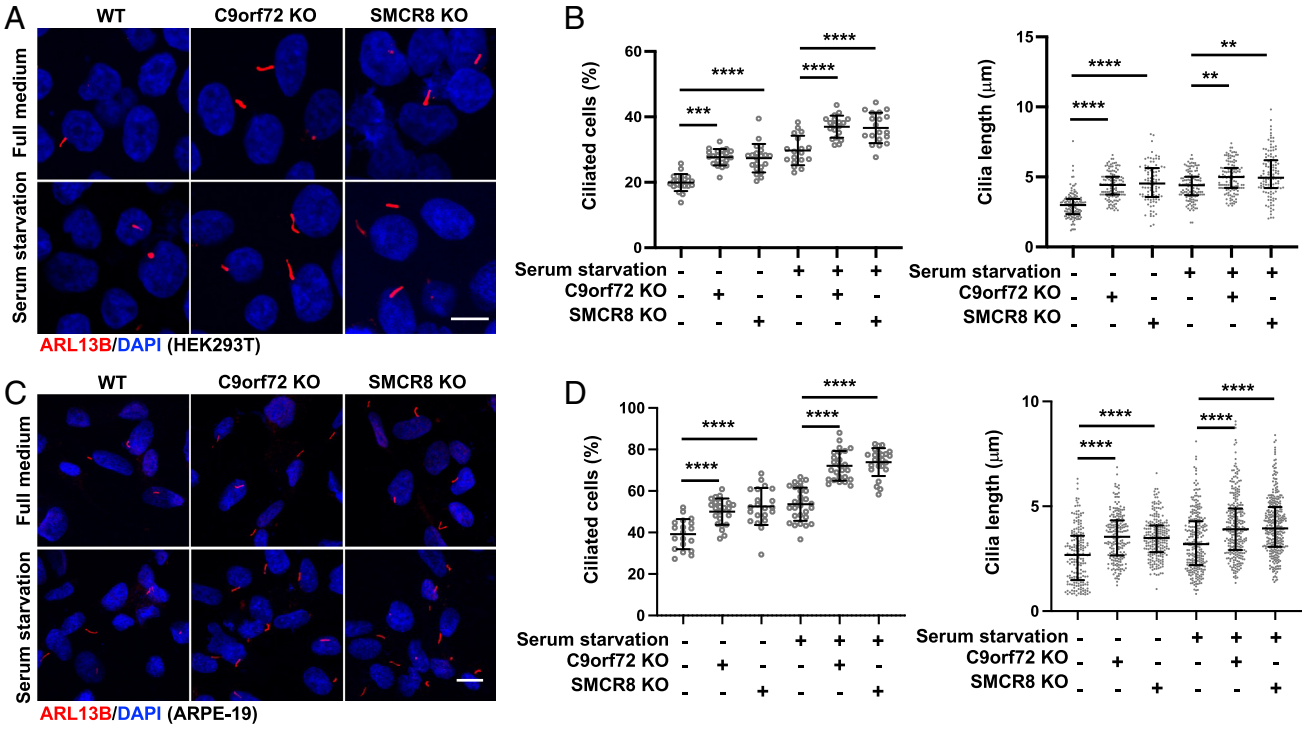

Fig. 1. Knocking out C9orf72 or SMCR8 enhances primary ciliogenesis. Representative immunofluorescence images and statistics analysis of cilia from wild-type (WT), C9orf72-knockout (C9KO), and SMCR8 knockout (S8KO) HEK293T cells incubated with or without serum for 16 h (*A* and *B*) or ARPE-19 cells incubated with or without serum for 24 h (*C* and *D*). The percentage of ciliated cells (*Left*) and the cilium length (*Right*) of HEK293T cells (*B*) or ARPE-19 cells (*D*) based on the data presented in (*A*) or (*C*). Scale bars, 10 μm. Data from three experiments with >200 cells were presented as the mean with SD for incidence and median with interquartile range for length. Significance was determined by one-way ANOVA followed by Tukey's multiple comparisons test for incidence and Dunn's nonparametric test for length (**P < 0.01; ***P < 0.001; ****P < 0.0001).

C9orf72 or SMCR8 in cells, respectively (*SI Appendix*, Fig. S2 *E–L*). In contrast, overexpression of C9orf72 in S8KO cells did not restore the phenotypes of the primary cilium due to SMCR8 knockout, and vice versa (Fig. 2 *A–H*), indicating that C9orf72 and SMCR8 synergically suppressed primary ciliognesis.

The GAP Activity of the C9orf72–SMCR8 Complex Is Required for Primary Ciliogenesis Suppression. To explore the mechanism by which the C9orf72–SMCR8 complex suppresses primary ciliogenesis, we first assessed the effect of knocking out C9orf72 and SMCR8 on the cell cycle since the primary cilium is highly associated with the cell cycle and mutually exclusive with cell division (46). The results showed that neither C9orf72 nor SMRC8 KO affected the cell cycle (*SI Appendix*, Fig. S3 *A* and *B*).

Ciliogenesis requires intraflagellar transport (IFT) (56). IFT proteins are necessary for the movement of IFT particles and are critical for ciliogenesis (56). Hence, we then examined whether C9KO and S8KO cells showed differences in the expression levels or localization of key IFT proteins (IFT20, IFT74, and IFT88) (57). The immunofluorescence staining and western blot results showed that neither C9orf72 nor SMCR8 KO changed the expression levels or localization of IFT proteins (*SI Appendix*, Fig. S3 *C–F*).

Given that the C9orf72–SMCR8 complex shows GAP activity for RAB8A/11A and Arf1/5/6 (18, 19), we proposed that the GAP activity of the C9orf72–SMCR8 complex is critical for inhibiting ciliogenesis. Arg147 of SMCR8 has been shown to be necessary for the GAP activity of the C9orf72–SMCR8 complex (18, 19). Therefore, SMCR8^{R147A}, a mutant lacking GAP activity, was generated to test our hypothesis. Compared with overexpression of WT SMCR8, overexpression of SMCR8^{R147A} in S8KO HEK293T and S8KO ARPE-19 cells had little effect on either the incidence of ciliogenesis or the average cilium length (Fig. 3 *A–D*), indicating that the GAP activity of the C9orf72–SMCR8 complex is required for the suppression of ciliogenesis.

Collectively, these data suggested that the GAP activity of the C9orf72–SMCR8 complex is necessary for the suppression of primary ciliogenesis, especially under serum starvation conditions.

The C9orf72–SMCR8 Complex Suppresses Primary Ciliogenesis as a GAP for RAB8A. Many RABs, including RAB5A, RAB8A, RAB10, RAB11, RAB17, and RAB23, have been suggested to be involved in primary ciliogenesis (58). Using a bioluminescence-based GTPase activity assay (18), we found that the C9orf72–SMCR8 complex showed GAP activity against most of the aforementioned RABs, except RAB23 (*SI Appendix*, Fig. S4*A*). Therefore, we investigated whether overexpression of the six RABs would affect primary ciliogenesis. The results indicated that RAB8A significantly increased both the incidence and length of the primary cilium (*SI Appendix*, Fig. S4 *B* and *C*). Importantly, only RAB8A localized to the primary cilium (*SI Appendix*, Fig. S4*B*). As expected, overexpression of ARF1/5/6 did not affect the primary cilium (*SI Appendix*, Fig. S4 *D* and *E*). Moreover, HEK293T cells and ARPE-19 cells with RAB8A KO showed a primary cilium phenotype similar to that of WT cells overexpressing C9orf72 or SMCR8 (Fig. 4 *A–D* and *SI Appendix*, Figs. S2 *A–D* and S5 *A* and *B*), and overexpressing the C9orf72–SMCR8 complex in RAB8A KO cells did not decrease ciliogenesis (Fig. 4 *A–D*), suggesting that the C9orf72–SMCR8 complex-RAB8A axis is the major regulatory pathway of primary cilium growth.

To further explore whether the C9orf72–SMCR8 complex inactivates RAB8A in cells, C9orf72–SMCR8/C9orf72–SMCR8^{R147A} and RAB8A were coexpressed in HEK293T and ARPE-19 cells. The phenotypic change in the primary cilium caused by RAB8A overexpression was counteracted by C9orf72–SMCR8 overexpression but not by C9orf72–SMCR8^{R147A} overexpression, indicating that the C9orf72–SMCR8 complex inactivates RAB8A as a GAP for RAB8A (*SI Appendix*, Fig. S5 *C–F*). We next investigated whether the C9orf72–SMCR8 complex shows GAP activity for RAB8A in cells using an in vivo GAP assay (59). In this assay, the effector proteins of RAB8A, optineurin (OPTN) (60), and EHBP1 (61), which can interact only with active RAB8A (RAB8A^{GTP}), were used as bait to quantify the levels of RAB8A^{GTP} in cells. Overexpression of RAB8A GAP in cells was expected to decrease the amount of RAB8A^{GTP} recruited by RAB8A effector proteins. In C9KO and S8KO cells, the amount of RAB8A immunoprecipitated by OPTN was increased by ~50% compared with that in WT cells (Fig. 4 *E* and *F*). Moreover, the amount of RAB8A immunoprecipitated by OPTN was decreased by ~two-fold in cells overexpressing C9orf72–SMCR8 compared with cells overexpressing C9orf72–SMCR8^{R147A} (Fig. 4 *G* and *H*). A similar phenotype was observed when purified EHBP1 was used as bait for RAB8A^{GTP} (*SI Appendix*, Fig. S5 *G–J*). Together, these observations suggested that the C9orf72–SMCR8 complex is a GAP for RAB8A in cells.

Collectively, the results indicated that the C9orf72–SMCR8 complex is a GAP for RAB8A in cells and that the C9orf72–SMCR8 complex suppresses primary ciliogenesis via its RAB8A GAP function.

The C9orf72–SMCR8 Complex Regulates the Localization of RAB8A to the Primary Cilium. The ciliary localization of RAB8A is critical for assembly of the primary cilium (42, 43); hence, we investigated whether the inactivation of RAB8A mediated by the C9orf72–SMCR8 complex disrupts RAB8A ciliary localization. Regardless of whether the cells were cultured with or without serum, more RAB8A localized to the primary cilium in C9KO or S8KO cells than in WT cells (Fig. 5 *A* and *B* and *SI Appendix*, Fig. S6 *A* and *B*). In addition, overexpressing C9orf72–SMCR8, but not C9orf72–SMCR8^{R147A}, decreased the localization of RAB8A to the primary cilium in cells cultured with or without serum (Fig. 5 *C* and *D* and *SI Appendix*, Fig. S6*C*). In general, the increase in cilium-localized RAB8A conferred by C9orf72 KO or SMCR8 KO promoted the incidence and length of the primary cilium (Fig. 5 *A* and *B* and *SI Appendix*, Fig. S6 *A* and *B*).

Since RAB8A also participates in trafficking in the Golgi and during exocytosis (35), we investigated whether the C9orf72–SMCR8 complex regulates the localization of RAB8A to the Golgi and PM. The results indicated that the localization of RAB8A to the Golgi and PM was not changed in the C9KO or S8KO cells compared with the WT cells (*SI Appendix*, Fig. S7 *A–D*).

Together, these results suggested that the C9orf72–SMCR8 complex mainly regulates the localization of RAB8A to the primary cilium via its RAB GAP function.

The Structural and Biochemical Basis for the RAB8A GAP Function of the C9orf72–SMCR8 Complex. To elucidate the mechanism by which the C9orf72–SMCR8 complex interacts with RAB8A and stimulates RAB8A GTPase activity, we tried to solve the structure of the C9orf72–SMCR8–RAB8A complex; however, the interaction of the C9orf72–SMCR8 complex with RAB8A was transient, and we could not obtain a stable C9orf72–SMCR8–RAB8A complex. Alternatively, a structural model of the C9orf72–SMCR8–RAB8A complex was generated on the basis of the C9orf72–SMCR8 complex structure (18) and C9orf72–SMCR8–Arf complex structure (Fig. 6*A*) (28). In the structural model, the tip of the C9orf72 β2–β3 loop (C9^{loop}) is inserted into a conserved hydrophobic pocket on RAB8A, which consists of F45, W62, and Y77 (Fig. 6*B*) and is referred to as the hydrophobic triad (62). Moreover, the β1–β2 loop (S8^{loop1}), α1–β3 loop (S8^{loop2}), and arginine finger loop in SMCR8 extend toward switch 2, switch 1,

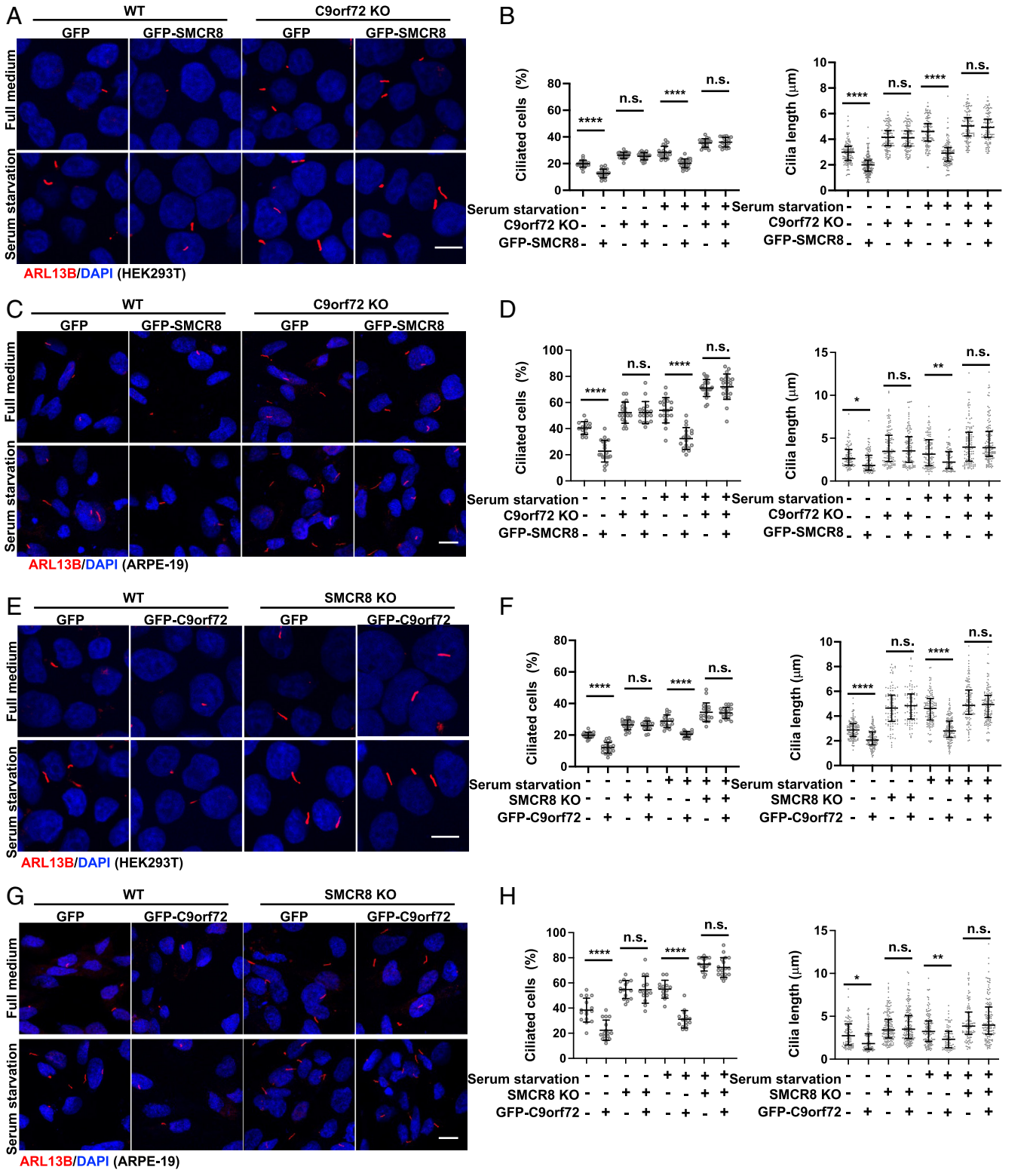

Fig. 2. The C9orf72–SMCR8 complex suppresses primary ciliogenesis. Representative immunofluorescence images and statistics analysis of cilia from WT and C9KO HEK293T cells (*A* and *B*) or ARPE-19 cells (*C* and *D*) transfected with GFP or GFP-SMCR8 plasmids and then incubated with or without serum for 16 h (*A*) or 24 h (*C*). The percentage of ciliated cells (*Left*) and the cilium length (*Right*) of HEK293T cells (*B*) or ARPE-19 cells (*D*) based on the data presented in (*A*) or (*C*). WT and S8KO HEK293T cells (*E* and *F*) or ARPE-19 cells (*G* and *H*) were transfected with GFP and GFP-C9orf72 plasmids and then incubated with or without serum for 16 h (*E*) or 24 h (*G*). The percentage of ciliated cells (*Left*) and the cilium length (*Right*) of HEK293T cells (*F*) or ARPE-19 cells (*H*) based on the data presented in (*E*) or (*G*). Scale bars, 10 μm. Data from three experiments with >200 cells were presented as the mean with SD for incidence and median with interquartile range for length. Significance was determined by one-way ANOVA followed by Tukey's multiple comparisons test for incidence and Dunn's nonparametric test for length (*P < 0.05; **P < 0.01; ****P < 0.0001; n.s. = not significant).

and the γ-phosphate group of the GTP of RAB8A, respectively (Fig. 6*C*). To assess the effect of the $C9^{loop}$ and $S8^{loop1/2}$ on the GAP function of the C9orf72–SMCR8 complex, five mutants, $C9orf72^{W33A}$, $C9orf72^{D34A}$, $C9orf72^{I71R}$, $SMCR8^{loop1}$ (in which residues 61-80 of SMCR8 were replaced with 2 pairs of GS), and $SMCR8^{loop2}$ (in which residues 105–15 of SMCR8 were replaced

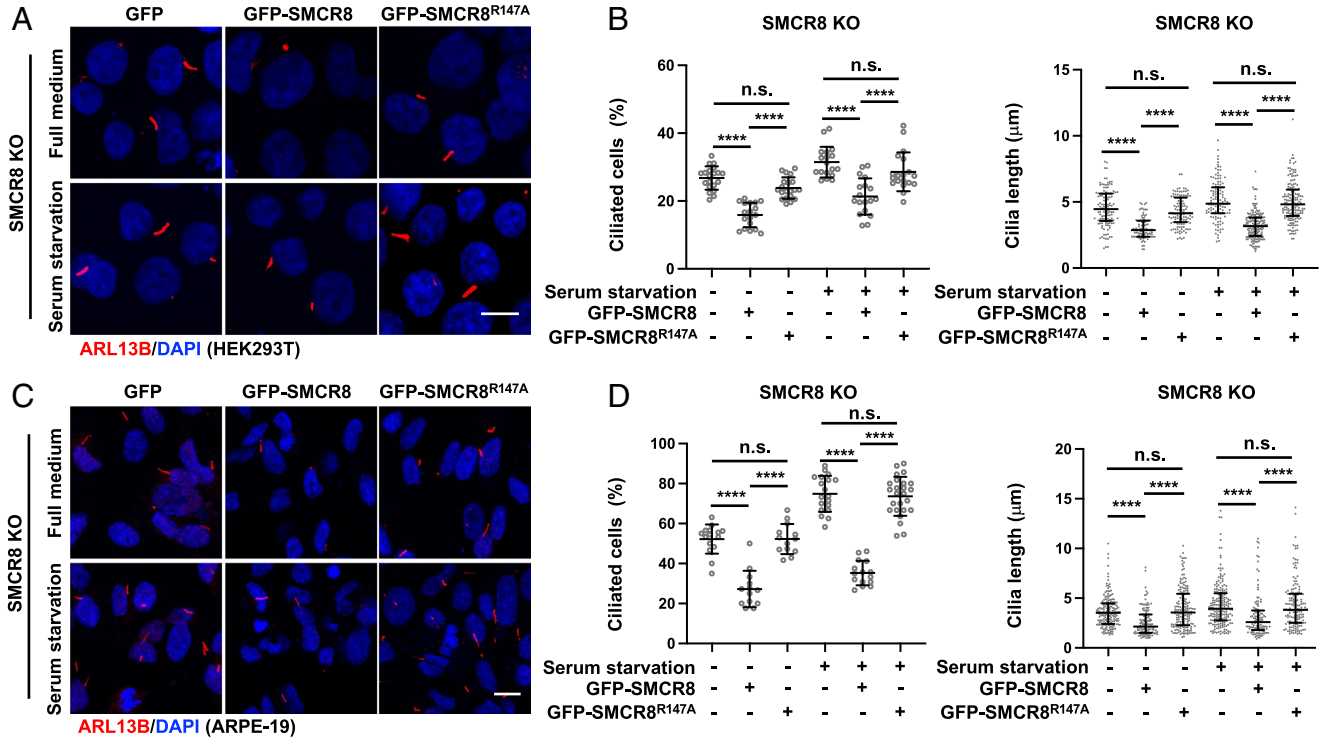

Fig. 3. GAP activity of the C9orf72–SMCR8 complex is essential for primary ciliogenesis suppression. Representative immunofluorescence images and statistics analysis of cilia from S8KO HEK293T cells (*A* and *B*) or ARPE-19 cells (*C* and *D*) transfected with GFP, GFP-SMCR8, or GFP-SMCR8^{R147A} and then incubated with or without serum for 16 h (*A*) or 24 h (*C*). The percentage of ciliated cells (*Left*) and the cilium length (*Right*) of HEK293T cells (*B*) or ARPE-19 cells (*D*) based on the data presented in (*A*) or (*C*). Scale bars, 10 μm. Data from three experiments with >200 cells were presented as the mean with SD for incidence and median with interquartile range for length. Significance was determined by one-way ANOVA followed by Tukey's multiple comparisons test for incidence and Dunn's nonparametric test for length (****$P < 0.0001$; n.s. = not significant).

with 5 pairs of GS), were generated. Notably, C9orf72 point mutants were generated according to a previous study (28). All five mutants almost lost the RAB8A GAP activity observed for the WT C9orf72–SMCR8 complex (Fig. 6*D*).

Next, using a pulldown assay, we further explored whether the five mutants would disturb the ability of the C9orf72–SMCR8 complex to bind RAB8A or its GAP activity for RAB8A. Interestingly, unlike the WT complex, the C9orf72^{W33A}–SMCR8 and C9orf72^{D34A}–SMCR8 complexes showed negligible interactions with RAB8A, while the C9orf72^{I71R}–SMCR8 complex showed a ~50% lower binding affinity for RAB8A (Fig. 6 *E* and *F*); however, SMCR8^{loop1}, SMCR8^{loop2}, and SMCR8^{R147A} did not affect the binding of the C9orf72–SMCR8 complex with RAB8A (Fig. 6 *E* and *F*). These observations indicated that the C9^{loop} is critical for binding of the C9orf72–SMCR8 complex with RAB8A and that the S8^{loop1} and S8^{loop2} are necessary for its GAP activity for RAB8A.

We then corroborated these findings in HEK293T cells. The phenotype of the primary cilium acquired after overexpressing RAB8A could not be counteracted by overexpressing the C9orf72^{W33A}–SMCR8 complex, the C9orf72^{D34A}–SMCR8 complex, the C9orf72^{I71R}–SMCR8 complex, or the C9orf72–SMCR8$^{loop1/2}$ complex (*SI Appendix*, Fig. S8*A*), confirming the biochemical observations in vitro.

Collectively, these data showed that the C9^{loop} plays a key role in the binding of the C9orf72–SMCR8 complex with RAB8A, and that the arginine finger loop and S8$^{loop1/2}$ contribute to the GAP activity of the C9orf72–SMCR8 complex.

The C9orf72–SMCR8 Complex Suppresses Primary Ciliogenesis In Vivo. To confirm that the C9orf72–SMCR8 complex suppresses primary ciliogenesis in vivo, we generated a C9KO mouse model (*SI Appendix*, Fig. S9*A*). Western blot analysis of multitissue samples taken from the C9KO mice suggested that C9orf72 was undetectable (*SI Appendix*, Fig. S9*B*). Since C9orf72 is highly expressed in the brain, spleen, kidney, and so on (63), we investigated whether the tissues from C9KO mice showed enhanced primary ciliogenesis. Analysis of mouse organ sections revealed that the incidence of primary ciliogenesis in the brain (neurons from the hippocampus, astrocytes from the cortex), kidney, and spleen was higher in the C9KO mice than in the WT mice (Fig. 7 *A*–*H* and *SI Appendix*, Fig. S9 *C* and *D*). Moreover, the measurable primary cilia in the organ sections obtained from the C9KO mice were obviously longer than those obtained from the WT mice (Fig. 7 *A*–*H* and *SI Appendix*, Fig. S9 *C* and *D*).

To confirm the observations in tissue sections, we also evaluated whether the cultured primary cells from C9KO mice showed enhanced primary ciliogenesis. Consistently, the primary astrocytes, neurons, primary kidney cells, and primary spleen cells isolated from the C9KO mice also showed a higher incidence of primary ciliogenesis and longer primary cilia than the respective data in WT mice; these differences were particularly salient under serum starvation conditions (*SI Appendix*, Fig. S10 *A*–*H*).

In summary, these results confirmed the phenotype of the primary cilium in C9KO cells, supporting the conclusion that the C9orf72–SMCR8 complex suppresses primary ciliogenesis.

Knocking Out C9orf72 or SMCR8 Increases Hh Signaling in NIH3T3 Cells. The formation of the primary cilium plays a crucial role in the activation of Hh signaling in vertebrates (47, 48). Hence, we evaluated the effect of knocking out of C9orf72 or SMCR8 on the Hh signaling. *Gli1* and *Ptch1* are the target genes of Hh signaling and thus are widely used to evaluate whether Hh signaling is activated (64, 65). NIH3T3 cells, a well-established tool for Hh signaling, with C9orf72 or SMCR8 knockout also

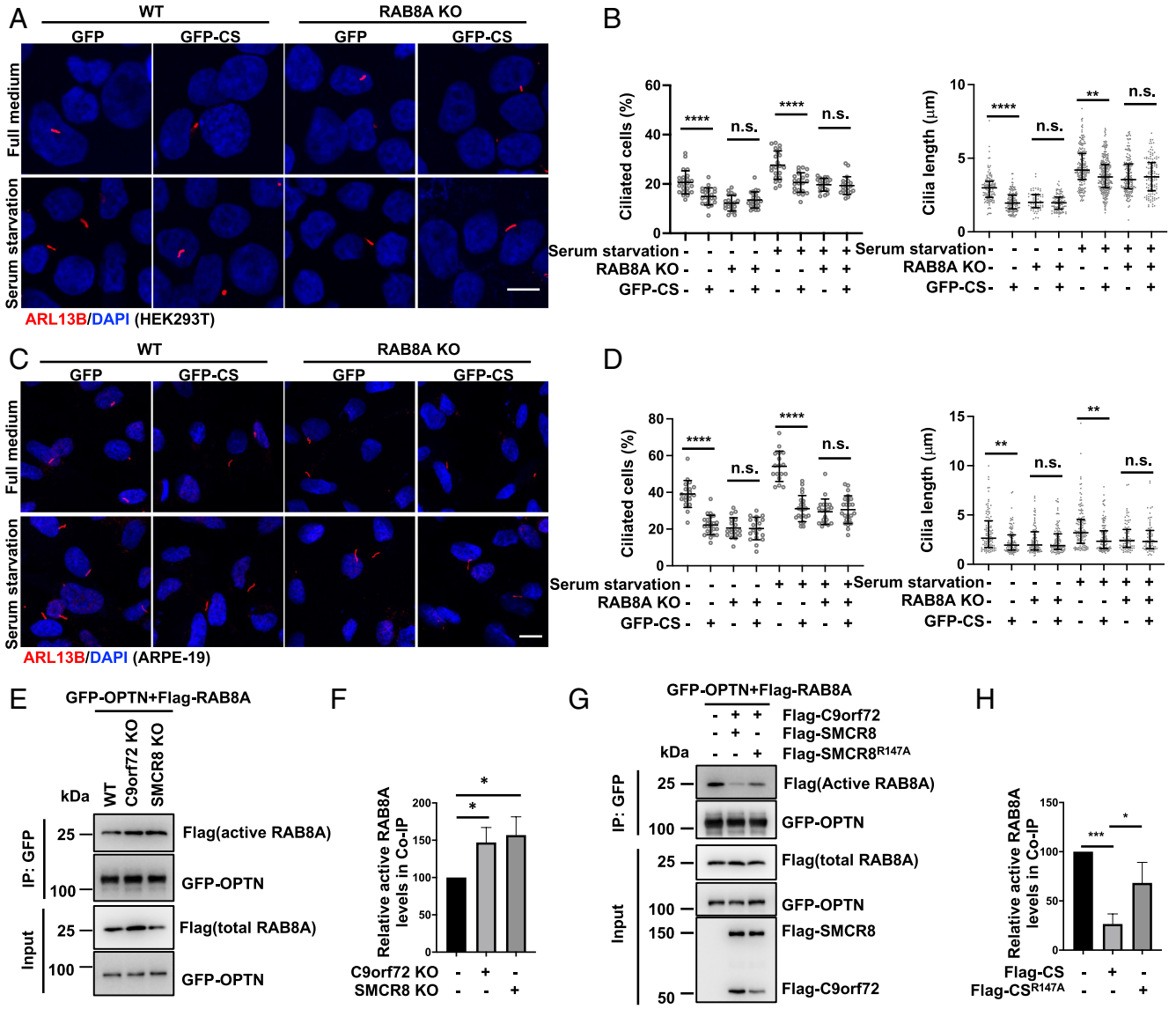

Fig. 4. The C9orf72–SMCR8 complex suppresses primary ciliogenesis via its RAB8A GAP function. Representative immunofluorescence images and statistics analysis of cilia from WT and RAB8A KO HEK293T cells (*A* and *B*) or ARPE-19 cells (*C* and *D*) transfected with GFP or cotransfected with GFP-C9orf72 and GFP-SMCR8 and then incubated with or without serum for 16 h (*A*) or 24 h (*C*). The percentage of ciliated cells (*Left*) and the cilium length (*Right*) of HEK293T cells (*B*) or ARPE-19 cells (*D*) based on the data presented in (*A*) or (*C*). Scale bars, 10 μm. Data from three experiments with >200 cells were presented as the mean with SD for incidence and median with interquartile range for length. Significance was determined by one-way ANOVA followed by Tukey's multiple comparisons test for incidence and Dunn's nonparametric test for length (**P < 0.01; ****P < 0.0001; n.s. = not significant). Western blot analysis of active form of RAB8A (RAB8A^{GTP}) bound to effector protein GFP-OPTN in WT, C9KO, and S8KO HEK293T cells cotransfected with GFP-OPTN and Flag-RAB8A (*E* and *F*) or WT HEK293T cells cotransfected with GFP-OPTN and Flag-RAB8A together with or without Flag-C9orf72 and Flag-SMCR8 or with the indicated mutant (*G* and *H*). Relative quantification of the data presented in (*E*) and (*G*) performed using ImageJ were shown in (*F*) and (*H*), respectively. The level of active RAB8A was normalized against OPTN. Error bars represented SD. Significance was determined by one-way ANOVA followed by Tukey's multiple comparisons test (n = 3, *P < 0.05; ***P < 0.001). Flag-CS: Flag-C9orf72+Flag-SMCR8 complex. Flag-CS^{R147A}: Flag-C9orf72+Flag-SMCR8^{R147A} complex.

showed enhanced primary ciliogenesis(*SI Appendix*, Fig. S11 *A–C*). We then stimulated the NIH3T3 cells using Shh and found that C9KO or S8KO significantly increased the Shh-induced expression of *Gli1* and *Ptch1* at both the mRNA and protein levels (Fig. 8 *A–C*). We also recovered C9orf72 or SMCR8 in C9KO or S8KO cells. As expected, wildtype C9orf72 or SMCR8 but not the loss-of-function mutants of C9orf72 (W33A, D34A) or SMCR8 (R147A) could rescue the Shh-induced expression of *Gli1* and *Ptch1* (Fig. 8 *D–G*). The results indicated that knocking out C9orf72 or SMCR8 enhances the primary ciliogenesis and thus increases the Hh signaling upon Shh induction.

The data obtained via biochemistry and cell biology experiments indicated that the C9orf72–SMCR8 complex is a negative regulator of the primary cilium and that this function depends on the GAP activity of the C9orf72–SMCR8 complex for RAB8A (*SI Appendix*, Fig. S12).

Discussion

To date, meaningful progress has been made in understanding the function of C9orf72, and C9orf72 has been suggested to be critical for many important biological processes. In this study, with multidisciplinary methods, we identified the primary cilium as a new organelle regulated by the C9orf72–SMCR8 complex and investigated the mechanism by which the C9orf72–SMCR8 complex mediates primary ciliogenesis.

Compared with WT cells, C9KO and S8KO cells showed longer primary cilia and a higher incidence of ciliogenesis, especially under

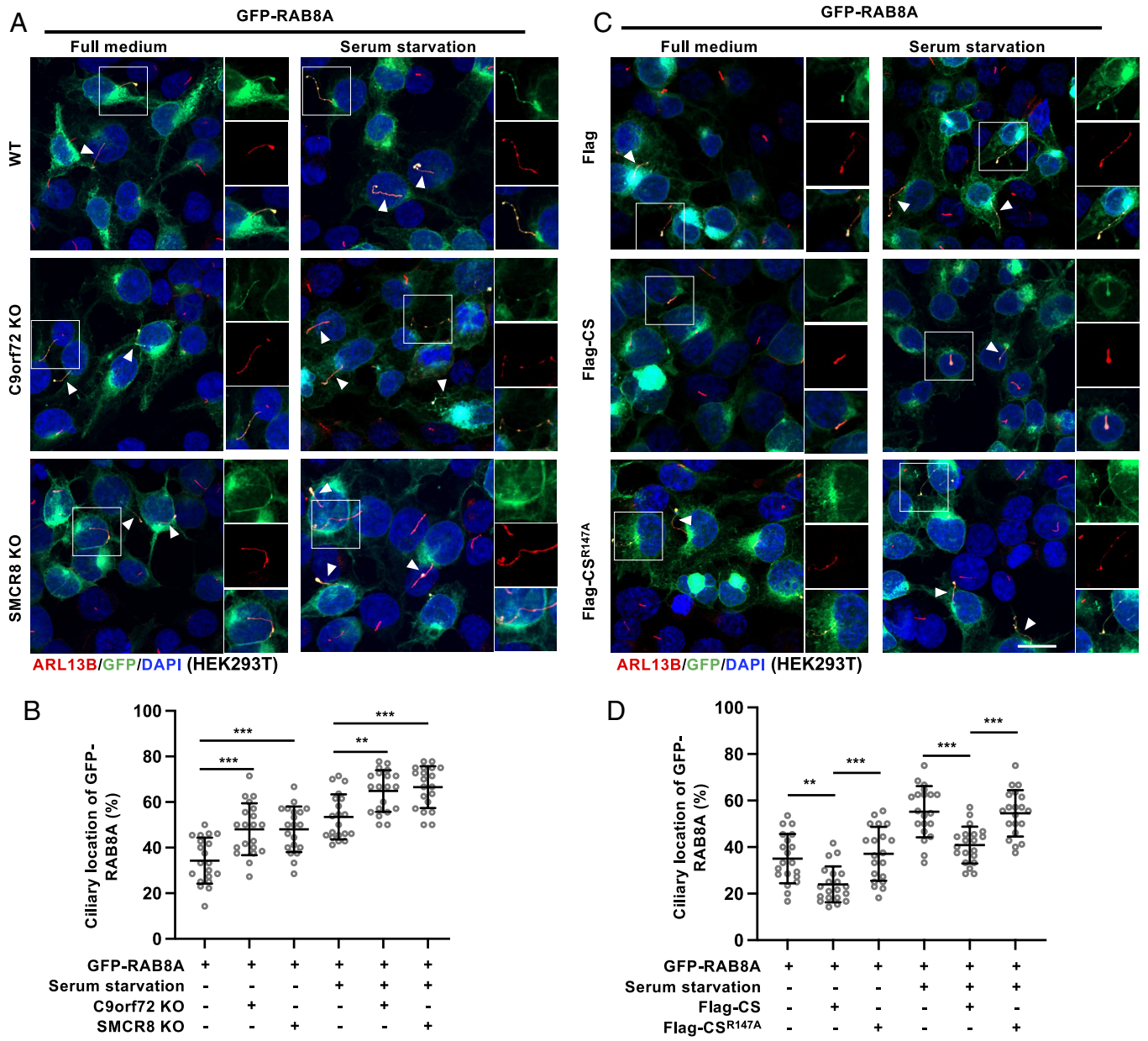

Fig. 5. The localization of RAB8A to the primary cilium is regulated by the C9orf72–SMCR8 complex. Representative confocal images and statistics analysis of cilia from WT, C9KO, and S8KO HEK293T cells transfected with GFP or GFP-RAB8A (*A* and *B*) or WT HEK293T cells cotransfected with GFP or GFP-RAB8A and Flag-C9orf72 + Flag-SMCR8 or the indicated mutant (*C* and *D*) and then incubated with or without serum for 16 h. Scale bars, 10 μm. The white arrows and the boxes indicate the colocalization of GFP-RAB8A with the primary cilium. The percentage of ciliary localization of GFP-RAB8A presented in (*A*) and (*C*) were shown in (*B*) and (*D*), respectively. Data from three experiments with >200 cells were presented as the mean with SD. Significance was determined by one-way ANOVA followed by Tukey's multiple comparisons test (**$P < 0.01$; ***$P < 0.001$).

serum-starvation conditions. This ciliary phenotype was similar to that observed in RAB8A-overexpressing cells. This observation indicates that the C9orf72–SMCR8 complex inhibits primary ciliogenesis and explains the in vitro results showing that RAB8A is a substrate of the C9orf72–SMCR8 GAP complex (18, 27). Mutagenesis and functional recovery experiments further suggested that the C9orf72–SMCR8 complex suppresses primary ciliogenesis in a manner dependent on RAB GAP activity.

We also confirmed that the C9orf72–SMCR8 complex inactivated RAB8A in cells. The level of RAB8A recruited by OPTN and EHBP1, which bind only with $RAB8A^{GTP}$, was increased by ~50% in C9KO or S8KO cells. Consistently, overexpressing C9orf72–SMCR8, but not C9orf72–$SMCR8^{R147A}$, decreased the level of RAB8A recruited by OPTN and EHBP1. These results have settled the disputed issue of whether RAB8A is a substrate of the C9orf72–SMCR8 GAP complex. The inability to reconstitute the C9orf72–SMCR8–RAB8A complex in vitro is probably due to the transient nature of the interactions between RAB8A and its GAPs; therefore, RAB8A–GAP complexes are unstable. This hypothesis is supported by the fact that no structure of RAB8A–GAP has been reported to date.

We have provided a detailed mechanism by which the C9orf72–SMCR8 complex stimulates GTP hydrolysis mediated by RAB8A. Consistent with a previous report (28), our study showed that the interaction of the C9orf72–SMCR8 complex with RAB8A required the $C9^{loop}$. Mutagenesis analysis revealed that W33 and D34 of C9orf72 are critical for the binding of the C9orf72–SMCR8 complex with RAB8A. The results presented here in

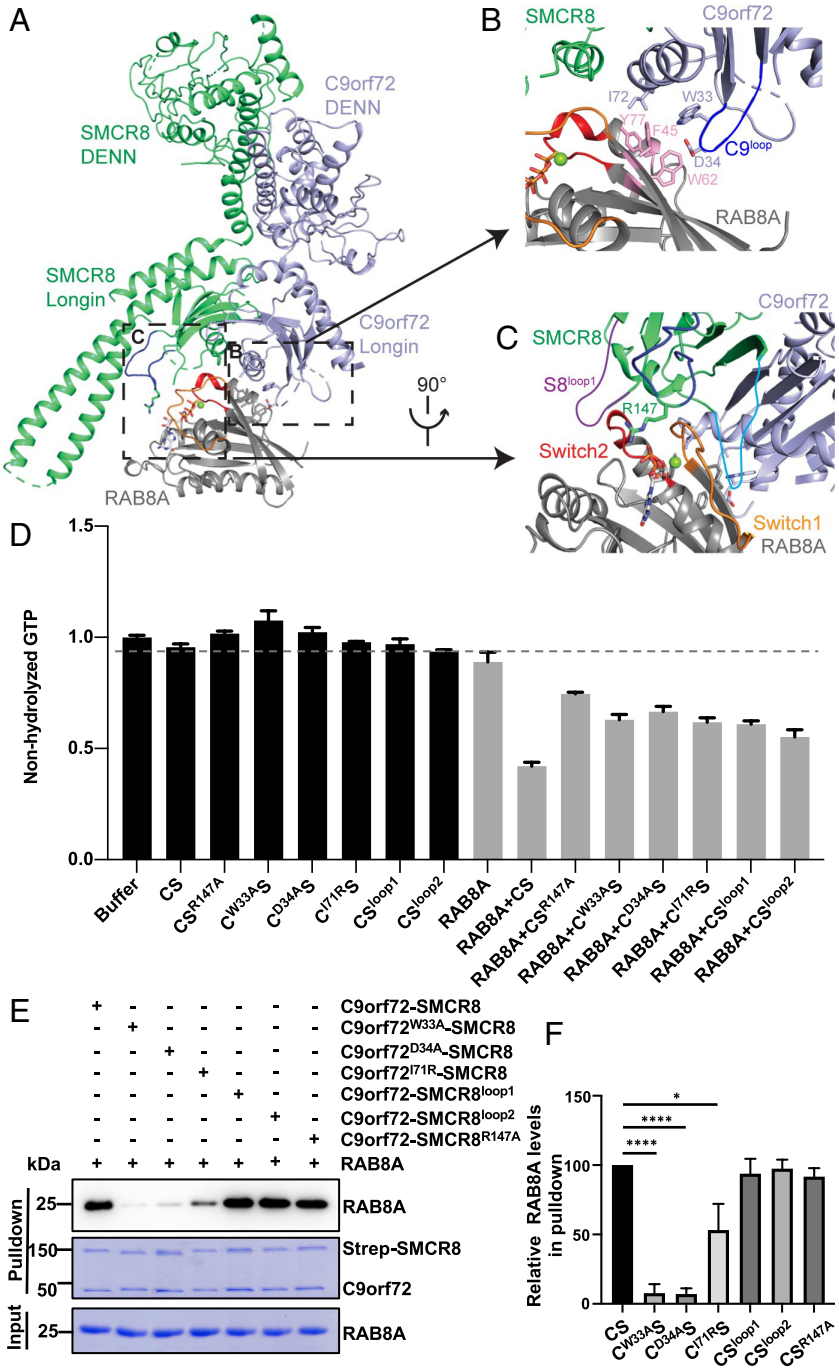

Fig. 6. Biochemical basis for the RAB8A GAP function of the C9orf72–SMCR8 complex. Overall structural model of the C9orf72-SMCR8-RAB8A complex generated based on the structural models of C9orf72-SMCR8-Arf1 (PDB ID: 7MGE), C9orf72-SMCR8 (PDB ID: 6LT0), and RAB8A (PDB ID: 6WHE) (*A*). Slate: C9orf72; green: SMCR8; gray: RAB8A. The black boxes showed details of the C9orf72 and RAB8A interface in (*B*) and the SMCR8 and RAB8A interface in (*C*). The hydrophobic triad, Switch 1 and switch 2 of RAB8A were colored pink, orange and red, respectively. The $C9^{loop}$, $S8^{loop1}$ and $S8^{loop2}$ were colored blue, purple and cyan, respectively. The GTP was shown as sticks. Green ball: Mg2+. The effect of C9orf72 and SMCR8 mutants on RAB8A stimulation or on RAB8A binding was analyzed using a GTPase-Glo assay (*D*) or a Strep-Tactin pulldown assay (*E*). Relative quantification of the data presented in (*E*) were shown in (*F*). CS: C9orf72-SMCR8; CS^{R147A}: C9orf72-$SMCR8^{R147A}$; CS^{loop1}: C9orf72-$SMCR8^{loop1}$; CS^{loop2}: C9orf72-$SMCR8^{loop2}$; $C^{W33A}S$: $C9orf72^{W33A}$-SMCR8; $C^{D34A}S$: $C9orf72^{D34A}$-SMCR8; C^{I71R} S: $C9orf72^{I71R}$–SMCR8. Error bars represented the SEM in (*D*) and SD in (*F*) based on three experiments. Significance was determined by one-way ANOVA followed by Tukey's multiple comparisons test (*$P < 0.05$; ****$P < 0.0001$).

combination with previous findings reported by the Hurley laboratory (28) suggest a conserved mechanism by which the $C9^{loop}$ plays a key role in substrate recognition by the C9orf72–SMCR8 GAP complex. Notably, we also found that the $S8^{loop1/2}$ was important for the RAB8A GAP activity of the C9orf72–SMCR8 complex but had little effect on the binding of C9orf72–SMCR8 to RAB8A. Most likely, the $S8^{loop1/2}$ facilitates stabilization of the switch 1/2 conformation in RAB8A (Fig. 6*C*). These observations advance our understanding of the catalytic mechanism through which the C9orf72–SMCR8 complex functions as a small GTPase GAP. Based on our data and those in previous reports, a functional model is proposed: C9orf72 is the substrate-binding subunit of the C9orf72–SMCR8 GAP complex (37, 38), while SMCR8 is the catalytic subunit of the C9orf72–SMCR8 GAP complex. Both subunits are necessary for the integral GAP activity of the C9orf72–SMCR8 complex.

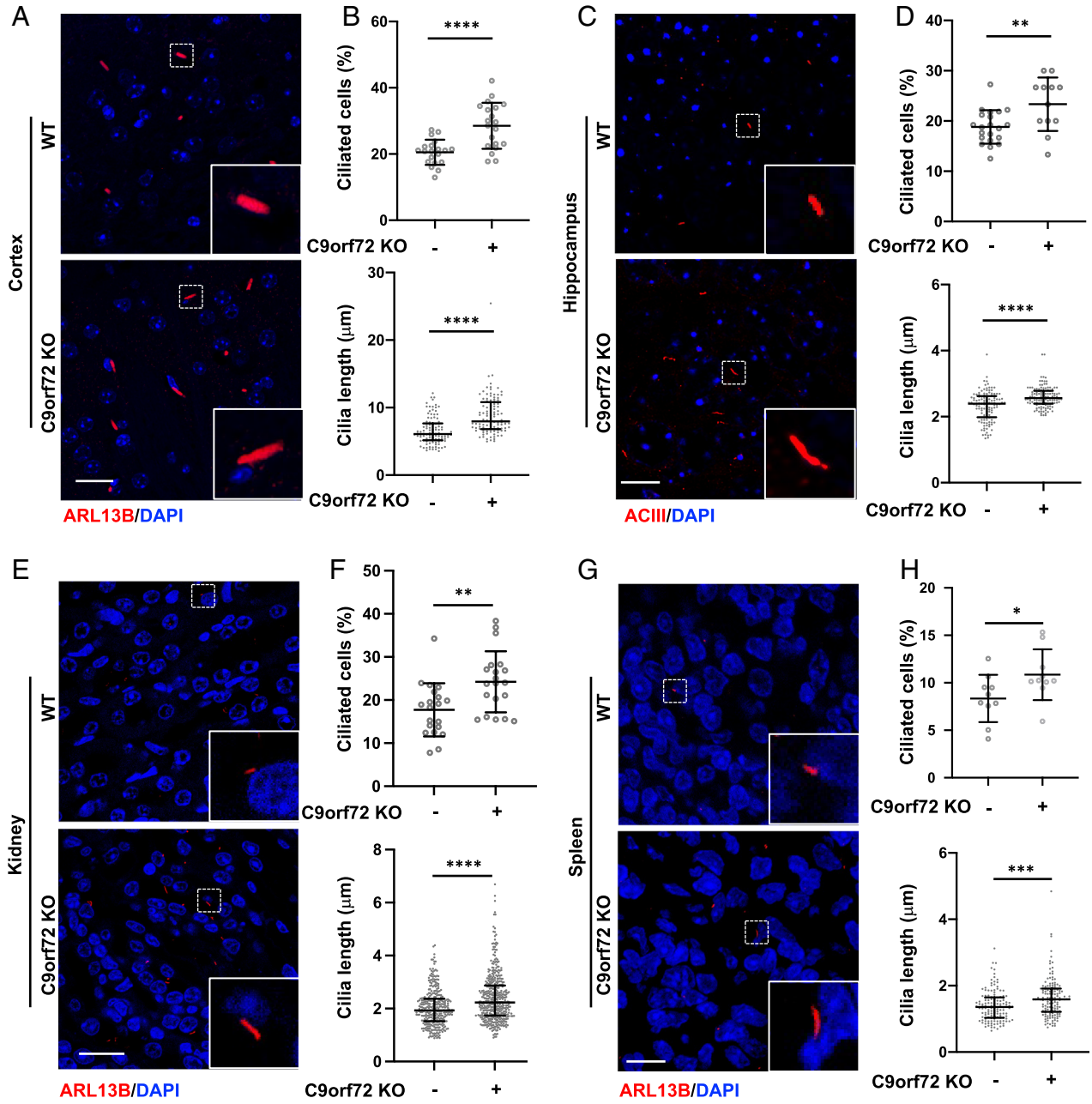

Fig. 7. The cells from C9KO mice show longer primary cilia. Representative confocal images and statistics analysis of cilia in brain cortex sections (*A* and *B*), brain hippocampus sections (*C* and *D*), kidney sections (*E* and *F*), and spleen sections (*G* and *H*) from both WT and C9KO mice. The percentage of ciliated cells (*Upper*) and length of the cilia (*Lower*) in cortex sections (*B*), brain hippocampus sections (*D*), kidney sections (*F*), and spleen sections (*H*) based on the data presented in (*A*), (*C*), (*E*) and (*G*), respectively. The primary cilia were stained with an anti-ARL13B (red) antibody or an anti-AC III (red) antibody. Scale bar, 20 μm (*A* and *E*) and 10 μm (*C* and *G*). Data from three experiments with >100 cells (*B* and *D*), >200 cells (*F*), and >130 cells (*H*) are presented as the mean with SD for incidence and median with interquartile range for length. Significance was determined by two-tailed Student's t test for incidence and Mann–Whitney test for length (*$P < 0.05$; **$P < 0.01$; ****$P < 0.0001$; ****$P < 0.0001$).

RAB8A can promote the elongation of the primary cilium by targeting vesicles to the primary cilium (42). In addition, many studies have suggested that RAB^{GTP}, but not RAB^{GDP}, localizes to primary cilia, promoting their elongation (40, 42, 43). Our data revealed that the localization of RAB8A to the primary cilium was increased in C9KO and S8KO cells (Fig. 5). Furthermore, overexpression of C9orf72–SMCR8 but not C9orf72–$SMCR8^{R147A}$ decreased the localization of RAB8A to the primary cilium, indicating that the C9orf72–SMCR8 complex drives a change from $RAB8A^{GTP}$ to $RAB8A^{GDP}$ via its GAP activity.

The C9orf72–SMCR8 complex forms a stable complex with WDR41, and mediated by PQLC2, the C9orf72–SMCR8–WDR41 complex is recruited to the lysosome, to which it binds under starvation conditions (12, 27, 28). Moreover, the primary cilium is actively extended under serum-starvation condition (40, 42, 45, 51). Hence, it is tempting to speculate that under serum-starvation conditions, the C9orf72–SMCR8–WDR41 complex is recruited to lysosomes through the interaction between WDR41 and PQLC2. In this scenario, the amount of the C9orf72–SMCR8 complex in the cytoplasm decreases, and the amount of $RAB8A^{GTP}$ increases, promoting primary ciliogenesis.

The inhibitory effect of the C9orf72–SMCR8 complex on primary ciliogenesis was confirmed using a C9KO mouse model. In the brain, spleen, and kidney, there were far more ciliated cells in the C9KO mice than in the WT mice, and the average lengths of the primary cilia on primary astrocytes/neurons/spleen/kidney

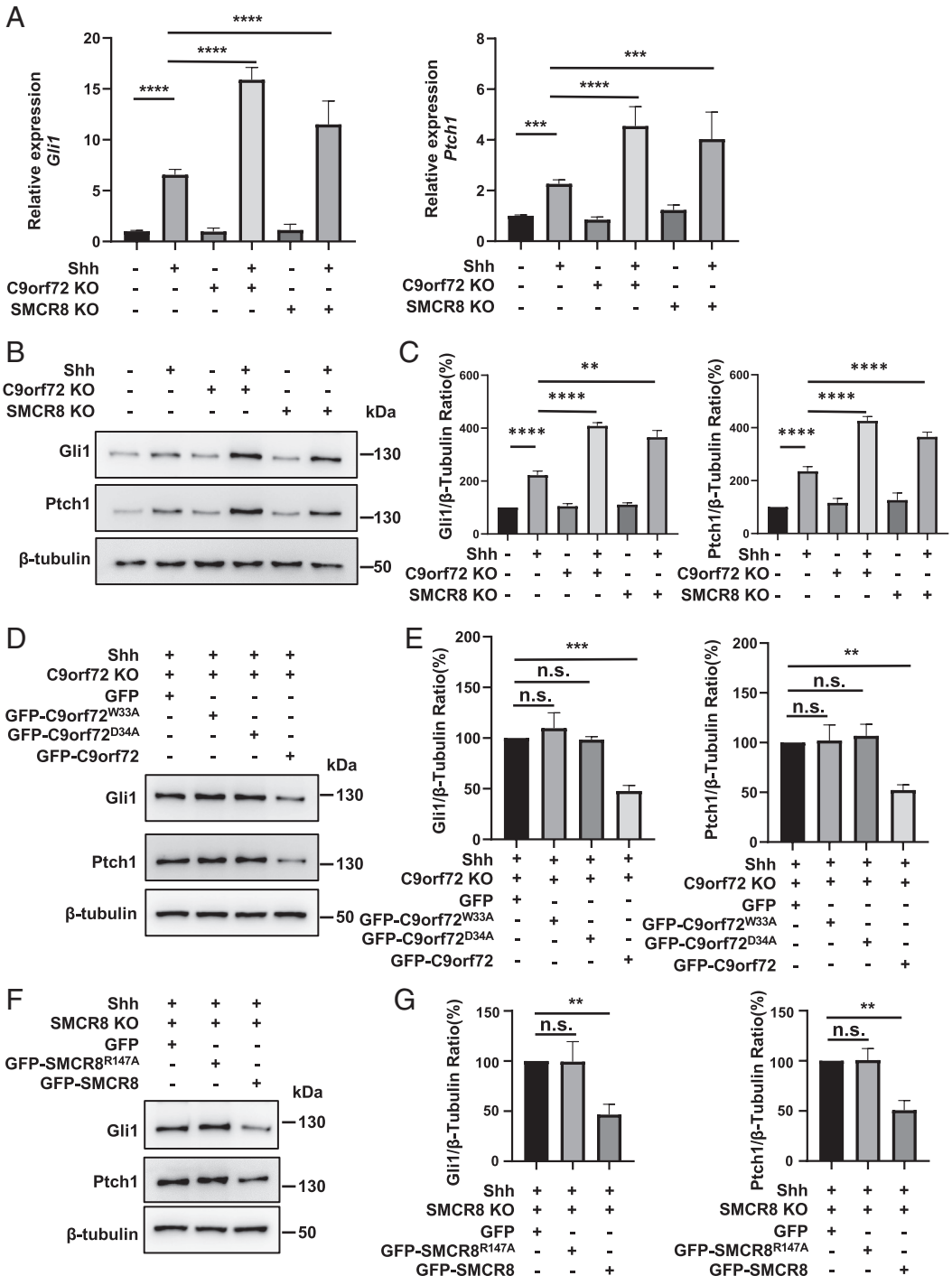

Fig. 8. Hh signaling is increased in C9orf72 KO and SMCR8 KO NIH3T3 cells. RT-qPCR analysis of mRNA levels of Gli1 and Ptch1 (*A*) or western blot analysis of protein levels of Gli1 and Ptch1 (*B* and *C*) in WT, C9KO, and S8KO cells with or without Shh treatment. Relative quantification (*C*) of the data presented in (*B*). The protein levels of Gli1 and Ptch1 in C9KO cells overexpressed GFP, GFP-C9orf72, GFP-C9orf72^{W33A} or GFP-C9orf72^{D34A} (*D* and *E*) or S8KO cells overexpressed GFP, GFP-SMCR8, or GFP- SMCR8R147A (*F* and *G*) in the presence of 1 μg/ml Shh for 24 h. Relative quantification of the data presented in (*D*) and (*F*) were shown in (*E*) and (*G*), respectively. Error bars represented SD. Significance was determined by one-way ANOVA followed by Tukey's multiple comparisons test (n = 3, $^{**}P < 0.01$; $^{***}P < 0.001$; $^{****}P < 0.0001$; n.s. = not significant).

cells from C9KO mice without serum starvation were similar to those of WT mice with serum starvation, indicating that the loss of C9orf72 function is associated with abnormal primary ciliogenesis.

C9orf72 is highly expressed in the brain, spleen, and kidney (63). Of note, C9KO mice showed abnormal enlargement of the spleen (8, 54). Moreover, in C9KO mice, inflammation in the intestine and kidney has been observed (14, 20). The primary cilium has been suggested to regulate the immune response (66), and a longer primary cilium has been observed in cells exposed to inflammatory cytokines (67). This evidence indicates that the spectrum of diseases caused by the loss of C9orf72 function might involve multiple systems or multiple organs and could be associated with abnormal primary cilia.

The primary cilium is necessary for Hh signaling in vertebrates, and the major players in Hh signaling, including Smo, Ptch, PKA, and Gli, are dynamically present in the primary cilium (47, 48). Importantly, Hh signaling is pivotal to embryonic development and

adult tissue homeostasis (47, 48). We found that cells with C9KO or S8KO showed enhanced primary ciliogenesis. Moreover, when C9orf72 or SMCR8 was knocked out, NIH3T3 cells were more sensitive to Shh signaling. Noteworthily, both the primary cilium and Hh signaling are highly related to the age-related brain disorders and neurodegenerative diseases (55, 64, 65, 68). Hence, the alteration caused by loss of C9orf72 function might be attributed to neurodegenerative diseases via primary ciliogenesis and Hh signaling.

Collectively, our data not only provide details regarding how the C9orf72–SMCR8 complex suppresses primary ciliogenesis through its RAB8A GAP function but also suggests a pathophysiologic mechanism underlying C9orf72-linked diseases. In the future, more effort should be made to investigate the relationship between primary ciliogenesis and C9orf72-related signaling pathways.

Materials and Methods

Generation of C9orf72-KO Mice and Cell Lines. For mice, Cas9 mRNA and sgRNA were generated by using in vitro transcript kits. All components were mixed well and injected into the cytoplasm of fertilized WT C57BL6 (B6) eggs. For cell lines, CRISPR/Cas9 method was performed as previously described (69).

Cell Culture and Primary Cilium Induction. Cell lines were cultured as recommended by the American Tissue Culture Collection. Primary cells were performed as described previously (70, 71). All cells were ciliated by serum starvation for different period of time.

Plasmids and Transfection. Genes were subcloned into indicated vectors using ClonExpress II One Step Cloning kit (Vazyme). The primers were designed using sdm-primer-v1.1 Python program (72). Transfection of plasmids was performed with Lipofectamine 2000 (Invitrogen).

Protein Expression and Purification. The EHBP1, RAB8A, and Shh were expressed in *E. coli* cells and purified by fast protein liquid chromatography. The C9orf72–SMCR8 complex was expressed and purified as previously described (18).

GTPase Activity Assay. GTPase activity assays were carried out using a GTPase-Glo assay kit (Promega, V7681) as previously described (18).

Immunoprecipitation and Pulldown Assays. For immunoprecipitation, cell lysates were incubated with GFP-Trap beads at 4 °C for 2 h. For pulldown assays, purified Strep-C9orf72–SMCR8 and RAB8A were incubated with Strep-Tactin beads at 4 °C for 1 h. The beads were eluted for western blot analysis.

Measuring Rab GAP Activity in Live Cells. The cleared lysates of cells cotransfected with Flag-RAB8A and GAP proteins were incubated with Strep-EHBP1$^{1060\text{-}1212}$ immobilized Strep-Tactin beads. The beads were eluted for subsequent western blotting.

Western Blotting. After being separated by sodium dodecyl sulfate–polyacrylamide gel electrophoresis (SDS-PAGE), transferred to the polyvinylidene difluoride (PVDF) membranes, blocking, stained with indicated primary antibodies, and incubated with appropriate secondary antibodies, target protein bands were detected by ChemiDoc MP Imaging System (Bio-Rad).

Immunofluorescence Assays. Fixed organs and cells incubated with the first antibodies and the Alexa 488- or Alexa 594-conjugated secondary antibodies were subjected to microscopes (ZEISS LSM 880 or N-STORM Super Resolution Microscopy System from Nikon) for imaging.

Flow Cytometric Analysis of the Cell Cycle. HEK29T cells were fixed and then suspended in PBS for flow cytometry analysis with ACEA NovoCyte Flow Cytometer (ACEA Biosciences, US).

Statistical Analysis. Data are reported as the means with SD/SEM or median with interquartile range. One-way ANOVA test and wo-tailed Student's *t* test in GraphPad Prism software (version 8.0) were used for multiple groups comparisons and two groups comparisons, respectively.

(Details of the materials and methods are included in *SI Appendix*).

Data, Materials, and Software Availability. All study data are included in the manuscript and *SI Appendix*.

ACKNOWLEDGMENTS. We thank Prof. Hongyuan Yang at the University of Texas Health Science Center and Prof. Guangshuo Ou at Tsinghua University for critically reading the manuscript. We thank Jie Zhang and Ling Bai at the Core Facility of West China Hospital, Sichuan University and Yang He and Ridong Huang at the Department of Respiratory and Critical Care Medicine, Targeted Tracer Research and Development Laboratory, West China Hospital, Sichuan University for providing immunofluorescence microscopy support. This work was supported by the NSFC grants 32071214 (S.Q.), the Natural Science Foundation of Sichuan, China 2022NSFSC0049 (S.Q.), NSFC grants 32022020 (K.L.), 32201025 (D.T.), and 31970693 (K.L.), and the 1·3·5 Project for Disciplines of Excellence, West China Hospital, Sichuan University [ZYYC20016 (S.Q.), ZYYC20015 (K.L.), ZYGD18011 (Hong Li), and ZYJC18015 (K.W.)], and the Fundamental Research Funds for the Central Universities 2022SCU12041 (D.T.).

Author affiliations: [a]Department of Urology, Institute of Urology, State Key Laboratory of Biotherapy, West China Hospital, College of Life Sciences, Sichuan University, and National Collaborative Innovation Center, Chengdu 610041, People's Republic of China; [b]Institute of Psychiatry and Neuroscience, Xinxiang Medical University, Xinxiang 453000, People's Republic of China; [c]Laboratory of Aging Research and Cancer Drug Target, State Key Laboratory of Biotherapy and Cancer Center, National Clinical Research Center for Geriatrics, West China Hospital, Sichuan University, Chengdu 610041, People's Republic of China; [d]Division of Life Science, Center of Systems Biology and Human Health, The Hong Kong University of Science and Technology, Kowloon, Hong Kong Special Administrative Region, People's Republic of China; [e]Southern Marine Science and Engineering Guangdong Laboratory (Guangzhou), Guangzhou 511458, People's Republic of China; [f]HKUST-Shenzhen Research Institute, Nanshan, Shenzhen 518057, People's Republic of China; [g]Sichuan Real & Best Biotech Co., Ltd., Chengdu 610219, People's Republic of China; and [h]National Health Commission Key Lab of Transplant Engineering and Immunology, West China Hospital, Sichuan University, Chengdu 610041, People's Republic of China

1. M. DeJesus-Hernandez *et al.*, Expanded GGGGCC hexanucleotide repeat in noncoding region of C9ORF72 causes chromosome 9p-linked FTD and ALS. *Neuron* **72**, 245–256 (2011).
2. A. E. Renton *et al.*, A hexanucleotide repeat expansion in C9ORF72 is the cause of chromosome 9p21-linked ALS-FTD. *Neuron* **72**, 257–268 (2011).
3. A. R. Haeusler *et al.*, C9orf72 nucleotide repeat structures initiate molecular cascades of disease. *Nature* **507**, 195–200 (2014).
4. Y. Shi *et al.*, Haploinsufficiency leads to neurodegeneration in C9ORF72 ALS/FTD human induced motor neurons. *Nat. Med.* **24**, 313–325 (2018).
5. B. D. Freibaum *et al.*, GGGGCC repeat expansion in C9orf72 compromises nucleocytoplasmic transport. *Nature* **525**, 129–133 (2015).
6. Y. Lin *et al.*, Toxic PR poly-dipeptides encoded by the C9orf72 repeat expansion target LC domain polymers. *Cell* **167**, 789–802 e712 (2016).
7. R. Sivadasan *et al.*, C9ORF72 interaction with cofilin modulates actin dynamics in motor neurons. *Nat. Neurosci.* **19**, 1610–1618 (2016).
8. Q. Zhu *et al.*, Reduced C9ORF72 function exacerbates gain of toxicity from ALS/FTD-causing repeat expansion in C9orf72. *Nat. Neurosci.* **23**, 615–624 (2020).
9. M. Yang *et al.*, A C9ORF72/SMCR8-containing complex regulates ULK1 and plays a dual role in autophagy. *Sci. Adv.* **2**, e1601167 (2016).
10. C. Sellier *et al.*, Loss of C9ORF72 impairs autophagy and synergizes with polyQ Ataxin-2 to induce motor neuron dysfunction and cell death. *EMBO J.* **35**, 1276–1297 (2016).
11. Y. Zhang *et al.*, The C9orf72-interacting protein Smcr8 is a negative regulator of autoimmunity and lysosomal exocytosis. *Genes Dev.* **32**, 929–943 (2018).
12. G. Talaia, J. Amick, S. M. Ferguson, Receptor-like role for PQLC2 amino acid transporter in the lysosomal sensing of cationic amino acids. *Proc. Natl. Acad. Sci. U.S.A.* **118**, e2014941118 (2020).
13. J. D. Lai, J. K. Ichida, C9ORF72 protein function and immune dysregulation in amyotrophic lateral sclerosis. *Neurosci. Lett.* **713**, 134523 (2019).
14. M. E. McCauley *et al.*, C9orf72 in myeloid cells suppresses STING-induced inflammation. *Nature* **585**, 96–101 (2020).
15. S. Xiao, P. M. McKeever, A. Lau, J. Robertson, Synaptic localization of C9orf72 regulates post-synaptic glutamate receptor 1 levels. *Acta Neuropathol. Commun.* **7**, 161 (2019).
16. D. Lall *et al.*, C9orf72 deficiency promotes microglial-mediated synaptic loss in aging and amyloid accumulation. *Neuron* **109**, 2275–2291.e8 (2021).
17. T. P. Levine, R. D. Daniels, A. T. Gatta, L. H. Wong, M. J. Hayes, The product of C9orf72, a gene strongly implicated in neurodegeneration, is structurally related to DENN Rab-GEFs. *Bioinformatics* **29**, 499–503 (2013).
18. D. Tang *et al.*, Cryo-EM structure of C9ORF72-SMCR8-WDR41 reveals the role as a GAP for Rab8a and Rab11a. *Proc. Natl. Acad. Sci. U.S.A.* **117**, 9876–9883 (2020).
19. M. Y. Su, S. A. Fromm, R. Zoncu, J. H. Hurley, Structure of the C9orf72 ARF GAP complex that is haploinsufficient in ALS and FTD. *Nature* **585**, 251–255 (2020).
20. P. M. Sullivan *et al.*, The ALS/FTLD associated protein C9orf72 associates with SMCR8 and WDR41 to regulate the autophagy-lysosome pathway. *Acta Neuropathol. Commun.* **4**, 51 (2016).

21. D. Zhang, L. M. Iyer, F. He, L. Aravind, Discovery of novel DENN proteins: Implications for the evolution of eukaryotic intracellular membrane structures and human disease. *Front. Genet.* **3**, 283 (2012).
22. S. Yoshimura, A. Gerondopoulos, A. Linford, D. J. Rigden, F. A. Barr, Family-wide characterization of the DENN domain Rab GDP-GTP exchange factors. *J. Cell Biol.* **191**, 367–381 (2010).
23. X. Wu *et al.*, Insights regarding guanine nucleotide exchange from the structure of a DENN-domain protein complexed with its Rab GTPase substrate. *Proc. Natl. Acad. Sci. U.S.A.* **108**, 18672–18677 (2011).
24. Y. Aoki *et al.*, C9orf72 and RAB7L1 regulate vesicle trafficking in amyotrophic lateral sclerosis and frontotemporal dementia. *Brain* **140**, 887–897 (2017).
25. K. Shen *et al.*, Cryo-EM structure of the human FLCN–FNIP2–Rag–ragulator complex. *Cell* **179**, 1319–1329.e8 (2019).
26. R. E. Lawrence *et al.*, Structural mechanism of a Rag GTPase activation checkpoint by the lysosomal folliculin complex. *Science* **366**, 971–977 (2019).
27. D. Tang, J. Sheng, L. Xu, C. Yan, S. Qi, The C9orf72–SMCR8–WDR41 complex is a GAP for small GTPases. *Autophagy* **16**, 1542–1543 (2020).
28. M. Y. Su, S. A. Fromm, J. Remis, D. B. Toso, J. H. Hurley, Structural basis for the ARF GAP activity and specificity of the C9orf72 complex. *Nat. Commun.* **12**, 3786 (2021).
29. S. R. Pfeffer, Rab GTPase regulation of membrane identity. *Curr. Opin. Cell Biol.* **25**, 414–419 (2013).
30. H. Stenmark, Rab GTPases as coordinators of vesicle traffic. *Nat. Rev. Mol. Cell Biol.* **10**, 513–525 (2009).
31. H. Zhu *et al.*, Rab8a/Rab11a regulate intercellular communications between neural cells via tunneling nanotubes. *Cell Death Dis.* **7**, e2523 (2016).
32. S. Zhu *et al.*, Rab11a-Rab8a cascade regulates the formation of tunneling nanotubes through vesicle recycling. *J. Cell Sci.* **131**, jcs215889 (2018).
33. Q. Feng *et al.*, Disruption of Rab8a and Rab11a causes formation of basolateral microvilli in neonatal enteropathy. *J. Cell Sci.* **130**, 2491–2505 (2017).
34. G. F. Vogel *et al.*, Abnormal Rab11-Rab8-vesicles cluster in enterocytes of patients with microvillus inclusion disease. *Traffic* **18**, 453–464 (2017).
35. P. Khandelwal *et al.*, A Rab11a-Rab8a-Myo5B network promotes stretch-regulated exocytosis in bladder umbrella cells. *Mol. Biol. Cell* **24**, 1007–1019 (2013).
36. K. Furusawa *et al.*, Cdk5 regulation of the GRAB-mediated Rab8-Rab11 cascade in axon outgrowth. *J. Neurosci.* **37**, 790–806 (2017).
37. Y. Omori *et al.*, Elipsa is an early determinant of ciliogenesis that links the IFT particle to membrane-associated small GTPase Rab8. *Nat. Cell Biol.* **10**, 437–444 (2008).
38. A. Knodler *et al.*, Coordination of Rab8 and Rab11 in primary ciliogenesis. *Proc. Natl. Acad. Sci. U.S.A.* **107**, 6346–6351 (2010).
39. P. Satir, S. T. Christensen, Overview of structure and function of mammalian cilia. *Annu. Rev. Physiol.* **69**, 377–400 (2007).
40. P. Satir, L. B. Pedersen, S. T. Christensen, The primary cilium at a glance. *J. Cell Sci.* **123**, 499–503 (2010).
41. L. Djenoune *et al.*, Cilia function as calcium-mediated mechanosensors that instruct left-right asymmetry. *Science* **379**, 71–78 (2023).
42. M. V. Nachury *et al.*, A core complex of BBS proteins cooperates with the GTPase Rab8 to promote ciliary membrane biogenesis. *Cell* **129**, 1201–1213 (2007).
43. S. Yoshimura, J. Egerer, E. Fuchs, A. K. Haas, F. A. Barr, Functional dissection of Rab GTPases involved in primary cilium formation. *J. Cell Biol.* **178**, 363–369 (2007).
44. J. A. Follit, L. Li, Y. Vucica, G. J. Pazour, The cytoplasmic tail of fibrocystin contains a ciliary targeting sequence. *J. Cell Biol.* **188**, 21–28 (2010).
45. V. Singla, J. F. Reiter, The primary cilium as the cell's antenna: Signaling at a sensory organelle. *Science* **313**, 629–633 (2006).
46. J. J. Malicki, C. A. Johnson, The cilium: Cellular antenna and central processing unit. *Trends Cell Biol.* **27**, 126–140 (2017).
47. Y. Chen, J. Jiang, Decoding the phosphorylation code in Hedgehog signal transduction. *Cell Res.* **23**, 186–200 (2013).
48. Z. Anvarian, K. Mykytyn, S. Mukhopadhyay, L. B. Pedersen, S. T. Christensen, Cellular signalling by primary cilia in development, organ function and disease. *Nat. Rev. Nephrol.* **15**, 199–219 (2019).
49. L. Djenoune, K. Berg, M. Brueckner, S. Yuan, A change of heart: New roles for cilia in cardiac development and disease. *Nat. Rev. Cardiol.* **19**, 211–227 (2022).
50. P. Avasthi, R. L. Maser, P. V. Tran, Primary cilia in cystic kidney disease. *Results Probl. Cell Differ.* **60**, 281–321 (2017).
51. C. Miceli *et al.*, The primary cilium and lipophagy translate mechanical forces to direct metabolic adaptation of kidney epithelial cells. *Nat. Cell Biol.* **22**, 1091–1102 (2020).
52. L. Tereshko, G. G. Turrigiano, P. Sengupta, Primary cilia in the postnatal brain: Subcellular compartments for organizing neuromodulatory signaling. *Curr. Opin. Neurobiol.* **74**, 102533 (2022).
53. M. Mc Fie *et al.*, Ciliary proteins specify the cell inflammatory response by tuning NFkappaB signalling, independently of primary cilia. *J. Cell Sci.* **133**, jcs239871 (2020).
54. J. G. O'Rourke *et al.*, C9orf72 is required for proper macrophage and microglial function in mice. *Science* **351**, 1324–1329 (2016).
55. H. S. Dhekne *et al.*, A pathway for Parkinson's Disease LRRK2 kinase to block primary cilia and Sonic hedgehog signaling in the brain. *Elife* **7**, e40202 (2018).
56. J. L. Rosenbaum, G. B. Witman, Intraflagellar transport. *Nat. Rev. Mol. Cell Biol.* **3**, 813–825 (2002).
57. M. Taschner *et al.*, Intraflagellar transport proteins 172, 80, 57, 54, 38, and 20 form a stable tubulin-binding IFT-B2 complex. *EMBO J.* **35**, 773–790 (2016).
58. O. E. Blacque, N. Scheidel, S. Kuhns, Rab GTPases in cilium formation and function. *Small GTPases* **9**, 76–94 (2018).
59. R. M. Nottingham, S. R. Pfeffer, Measuring Rab GTPase-activating protein (GAP) activity in live cells and extracts. *Methods Mol. Biol.* **1298**, 61–71 (2015).
60. K. Hattula, J. Peranen, FIP-2, a coiled-coil protein, links Huntingtin to Rab8 and modulates cellular morphogenesis. *Curr. Biol.* **10**, 1603–1606 (2000).
61. A. Rai, N. Bleimling, I. R. Vetter, R. S. Goody, The mechanism of activation of the actin binding protein EHBP1 by Rab8 family members. *Nat. Commun.* **11**, 4187 (2020).
62. E. Merithew *et al.*, Structural plasticity of an invariant hydrophobic triad in the switch regions of Rab GTPases is a determinant of effector recognition. *J. Biol. Chem.* **276**, 13982–13988 (2001).
63. M. Uhlen *et al.*, Proteomics. Tissue-based map of the human proteome. *Science* **347**, 1260419 (2015).
64. M. Zhou, Y. Han, J. Jiang, The Pseudokinase Ulk4 promotes Shh signaling by regulating Stk36 ciliary localization and Gli2 phosphorylation. *eLife* **12**, RP88637 (2023).
65. S. Schmidt *et al.*, Primary cilia and SHH signaling impairments in human and mouse models of Parkinson's disease. *Nat. Commun.* **13**, 4819 (2022).
66. H. Baek *et al.*, Primary cilia modulate TLR4-mediated inflammatory responses in hippocampal neurons. *J. Neuroinflammation* **14**, 189 (2017).
67. A. K. Wann, M. M. Knight, Primary cilia elongation in response to interleukin-1 mediates the inflammatory response. *Cell Mol. Life Sci.* **69**, 2967–2977 (2012).
68. R. Ma, N. A. Kutchy, L. Chen, D. D. Meigs, G. Hu, Primary cilia and ciliary signaling pathways in aging and age-related brain disorders. *Neurobiol. Dis.* **163**, 105607 (2022).
69. L. Cong *et al.*, Multiplex genome engineering using CRISPR/Cas systems. *Science* **339**, 819–823 (2013).
70. R. Yang, E. Kong, J. Jin, A. Hergovich, A. W. Puschel, Rassf5 and Ndr kinases regulate neuronal polarity through Par3 phosphorylation in a novel pathway. *J. Cell Sci.* **127**, 3463–3476 (2014).
71. P. Yan *et al.*, Crosstalk of Synapsin1 palmitoylation and phosphorylation controls the dynamicity of synaptic vesicles in neurons. *Cell Death Dis.* **13**, 786 (2022).
72. C. Bi *et al.*, A python script to design site-directed mutagenesis primers. *Protein Sci.* **29**, 1054–1059 (2020).